Spots and turbulent domains in a model of transitional plane Couette flow

Paul Manneville

Laboratoire d'Hydrodynamique (LadHyX)
École polytechnique, F-91128 Palaiseau, France
e-mail: paul.manneville@ladhyx.polytechnique.frc - Web page: http://www.ladhyx.polytechnique.fr/

ABSTRACT

Introduction. The problem of the transition to turbulence is best understood in a globally supercritical context, e.g. for Rayleigh–Bénard convection. Difficulties arise for open flows that are mechanically stable (no inflection point in the base velocity profile), that is, boundary layer flows, plane Poiseuille flow or plane Couette flow (pCf). In that case the transition to turbulence can be direct from the laminar state and occur *via* spatiotemporal intermittency as discussed first by Pomeau [1] at a conceptual level. Subcriticality and coexistence of laminar and turbulent domains are the key features of the proposed scenario but, in practice, it is not easy to set experimental observations within that framework. A review of the work done on the pCf at Saclay has been given in the first part of a paper by Dauchot and myself [2]. Its second part was devoted to a presentation of preliminary simulation results on a model [3] mimicking the behavior of that flow. After a brief summary of this modeling attempt, I will describe new results about the growth of spots and turbulent domains that resemble what is observed experimentally and further raises new questions.

The model. The problem of how turbulence is sustained in wall flows is a difficult one that Waleffe approached by developing a Lorenz-like model in terms of ordinary differential equations [4] coupling the amplitudes of few Fourier modes, and accounting for the regeneration cycle of streaks and streamwise vortices supposed to play the principal role in the process. Though nontrivial solutions of the expected type are present in his model, such a low-dimensional approach is not satisfactory since it postulates periodic boundary conditions at a small distance that behave as confinement effects incompatible with the observed spatiotemporal evolution. In order to go beyond and, in some sense, to unfreeze the space dependence of the system, few years ago I developed a Swift–Hohenberg-like model, from which Waleffe's model can be recovered when his specific boundary conditions are imposed. In this model, the in-plane space (x, z) dependence is fully accounted for while the cross-stream (y) dependence is truncated, hence the term "2.5 dimensional" model. The base flow is taken[1] as $u = u_{\rm b} = \sin(\beta y)$ and "stress free" boundary conditions are assumed at $y = \pm 1$ which implies $\beta = \pi/2$ (the flow is driven by an appropriate body force). The perturbations are expanded as Fourier series in y with coefficients depending on x, z, and time t:

$$u' = U_0 + U_1 \sin(\beta y) + \sum_{k\geq 1} U_{2k} \cos(2k\beta y) + U_{2k+1} \sin((2k+1)\beta y) \qquad (1)$$

with similar expressions for v' and w'. Up to now only a consistent truncation at lowest order has been considered (subscripts 0 and 1). The Navier–Stokes equations for the perturbations then read:

- continuity equation:

$$\partial_x U_0 + \partial_z W_0 = 0 \qquad (2)$$

$$\partial_x U_1 + \partial_z W_1 = \beta V_1 \qquad (3)$$

[1] Velocities and lengths are scaled with the speed of the plates ΔU and the half gap h; the Reynolds number is then defined as $R = \Delta U h/\nu$, as usually done by experimentalists. Physically it would be more meaningful to choose a Reynolds number $\widetilde{R}$ based on the shear rate and the thickness of the layer, hence $\widetilde{R} = 4R$, in order to allow comparisons with other flows, e.g. Poiseuille or Couette–Taylor.

- x-component of the momentum equation (y independent projection):

$$\begin{aligned}\partial_t U_0 + U_0\partial_x U_0 + W_0\partial_z U_0 + \tfrac{1}{2}U_1\partial_x U_1 + \tfrac{1}{2}\beta V_1 U_1 + \tfrac{1}{2}W_1\partial_z U_1 \\ = -\partial_x P_0 - \tfrac{1}{2}\partial_x U_1 - \tfrac{1}{2}\beta V_1 + R^{-1}\Delta_2 U_0 \end{aligned} \quad (4)$$

where $\Delta_2 \equiv \partial_{xx} + \partial_{zz}$ and R is the Reynolds number. Similar equations are obtained for the other components of the momentum equation and the projections on $\sin(\beta y)$ and $\cos(\beta y)$.

In order to eliminate the pressure, stream functions and potentials are introduced such that $U_0 = -\partial_z\Psi_0$, $W_0 = \partial_x\Psi_0$, $U_1 = \partial_x\Phi_1 - \partial_z\Psi_1$, $W_1 = \partial_z\Phi_1 + \partial_x\Psi_1$, and $V_1 = (\Delta_2\Phi_1)/\beta$, which leads us to work with three nonlinear partial differential equations for three unknowns Ψ_0, Ψ_1, and Φ_1. The model respects the main characteristics of the problem (linear stability of base flow, appropriate structure for the nonlinear advection terms that conserve the kinetic energy, non-normality).

The results. Early numerical simulations were performed under conditions that correspond to experiments with a turbulent state prepared at high R and suddenly quenched at a lower R. They have shown the existence of transients similar to those observed in the laboratory for R below some The global stability threshold $R_{\rm g}$ and sustained turbulence above. In the model, $R_{\rm g}$ is of the order of 45 [2,3], whereas $R_g = 325$ in the laboratory experiments [2]. Results presented here refer to new simulations[2] obtained after several doublings of the system's linear size. They have shown that the statistical properties of the turbulent regime were extensive (turbulent energy per unit surface independent of size in the considered range) and confirmed previous findings about $R_{\rm g}$. Our unrealistically low value is likely to be related to the choice of stress-free boundary conditions (as for convection) and to the low order truncation that underestimates viscous dissipation.

Here we focus on the most recent numerical experiments dealing with spot growth and the coexistence of large turbulent and laminar domains. The initial conditions are derived from a previously obtained homogeneous turbulent regime at $R = 100$ by masking part of it in order to define the laminar region, i.e. setting to zero the fields ψ_0, ψ_1, and ϕ_1 outside domains of different shapes and connecting states smoothly at the boundary. Circular domains with small diameter served as initial conditions to study the nucleation of droplets. Bands, streamwise, spanwise, or oblique, were prepared to test the behavior of domain fronts between the laminar and turbulent states. Several values of the Reynolds number have been considered. Figure 1 displays the evolution of the energy contained in the spot developing from a small germ. As understood from the left panel, the spot decays for $R = 50$ and $R = 60$. The perturbation is thus insufficient to trigger the homogeneous turbulent regime otherwise observed for these values of R in the quench experiment. By contrast, the right panel shows that the developed regime is obtained for $R = 70$ after a transient in two steps. The initial growth stage resembles those for lower R but is now sufficiently powerful to give rise to a large domain of sustained turbulence. During the late stage this domain invades the whole system. Pictures of it at several times are displayed in Fig. 2.

The second experiment presented here focus more on the invasion stage and the problem of front propagation between the turbulent and laminar domains. Here we only display the case of spanwise bands. For $R = 70$, the width of the turbulent domain grows and the final state is the expected homogeneous turbulent state (see Fig. 3 in which the local kinetic energy contained in the perturbation is displayed in colors) whereas for $R = 50$ the band still widens but turbulence finally decays in much the same way as it does in the quench experiment. A crude, naive, but economic visualization of the fronts separating turbulent and laminar domains is displayed in Fig. 4: the local turbulent intensity is averaged over

[2]Pseudo-spectral code with alias removing, 1024×512 modes, $\delta x = \delta z = 0.125$ hence $L_x = 128$ and $L_z = 64$, second-order time integration with exact evaluation of linear terms and an Adams–Bashforth scheme for nonlinear terms.

the spanwise width of the system and this function of the remaining streamwise coordinate is further evaluated every $\delta t = 2.5$ from $t = 0$ to $t = 60$. The interesting result is obtained that the front moves faster for $R = 70$ than for $R = 50$, that in both cases the average turbulence intensity first decreases as the domain expands, but that it remains at a sufficiently high value to trigger the return to the uniformly turbulent regime when $R = 70$ while it eventually decays when $R = 50$.

Provisional conclusions. Beyond the qualitative restitution of the globally subcritical behavior already reported before [2,3], it should be remarked first that the model mimics the growth of turbulent spots or bands equally well. This suggests us to study in more detail how the initial growth stage depends on R and the initial shape/intensity of the perturbation, thus how the boundary of the attraction basin of the turbulent regime is approached. (Tumbling from this early stage to the invasion stage is still certainly dependent on the system's size.)

Though efforts should be made to improve the monitoring of front motion, interesting results have already be obtained, in particular that turbulence grow through advancing fronts but decay by local collapse rather than by receding fronts. This raises questions about one facet of Pomeau's conjecture [1] about the concrete applicability of the spatiotemporal intermittency scenario to the pCf case.

Interesting things happen in the model at unrealistically low values of R. Developing a Galerkin expansion on an appropriate polynomial basis apt to deal with the no slip boundary conditions at the moving plates is straightforward. However, for the moment I prefer to check the role of an increased cross-stream resolution by jumping to the next consistent modeling and adding two more fields, Ψ_2 and Φ_2, to Ψ_0, Ψ_1, and Φ_1. This implies taking into account some energy transfer towards smaller scales where dissipation is expected to take place, while keeping the focus on coherent structures at the scale of the gap between the plates. In this way many more individual mechanisms can be tested by manipulating the initial conditions in a controlled way. Finally, the breakdown of spiral turbulence in the case of counter rotating Taylor–Couette flow is very similar to that of transitional pCf and an adaptation of the present strategy is an appealing topic that I begin to consider in parallel.

Acknowledgements. Computer time has been provided by IDRIS (project CP6/1462). Olivier Dauchot and his collaborators at GIT-SPEC Saclay, Bruno Eckhart and his group in Marburg, Carlo Cossu, Laurette Tuckerman and Dwight Barkley are all thanked for interesting discussions related to this study. Work is currently developed in collaboration with two undergraduate students, Maher Lagha and Joachim Kruithof.

REFERENCES

[1] Y. Pomeau, Physica D **23** (1986) 3–11, and Section IV.4 in P. Bergé, Y. Pomeau, Ch. Vidal, *L'espace chaotique* (Hermann, Paris, 1998).

[2] P. Manneville & O. Dauchot, in *Coherent structures in classical systems*, D. Reguera, L.L. Bonilla, J.M. Rubi, eds. (Springer Verlag, 2001) pp. 58–79.

[3] P. Manneville & F. Locher, C. R. Acad. Sc. IIb - Mécanique **328** (2000) 159–164. P. Manneville, in *Advances in Turbulence VIII* C. Dopazo *el al.* (Eds), CIMNE, Barcelona 2000.

[4] F. Waleffe, Phys. Fluids **9** (1997) 883-900.

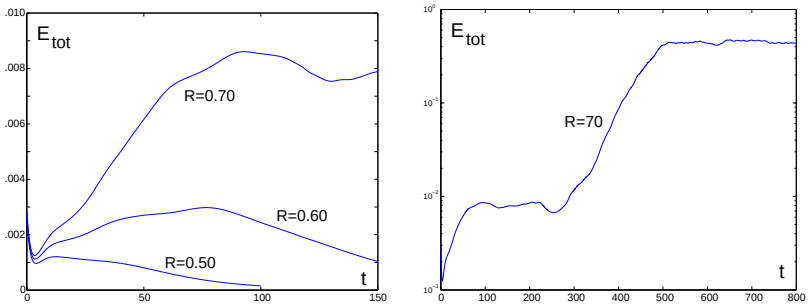

Fig. 1: Total energy contained in evolving turbulent spots; short term evolution for $R = 50, 60, 70$ (left) and transition to the sustained turbulent regime for $R = 70$ (right).

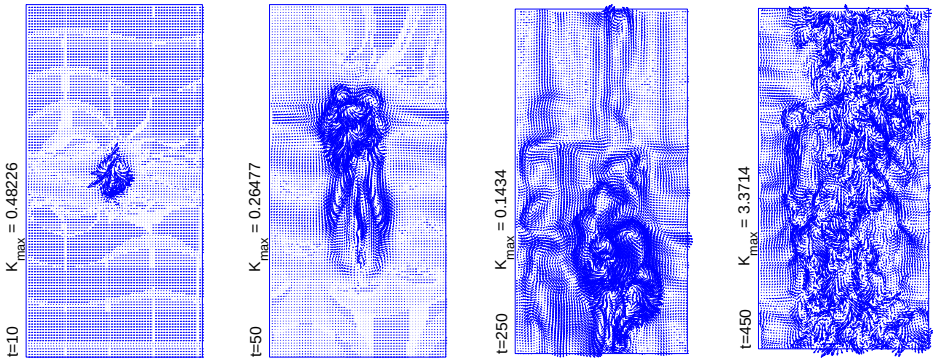

Fig. 2: Snapshots taken during the transition from a germ with $R = 70$. (Spanwise and streamwise coordinates horizontal and vertical, respectively.)

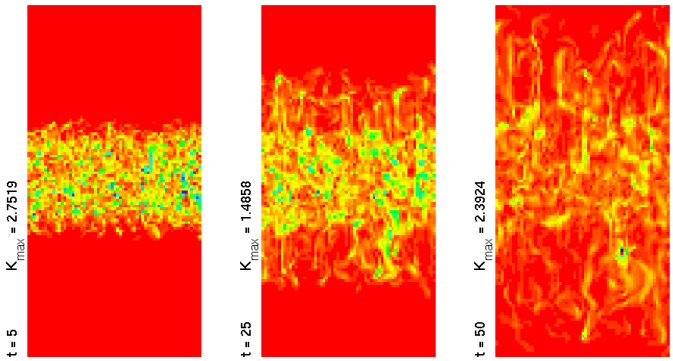

Fig. 3: Widening of a spanwise band for $R = 70$. (Coordinates as in Fig. 2.)

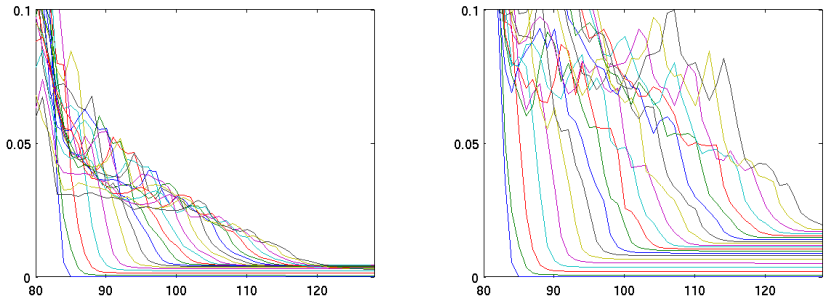

Fig. 4: Turbulence averaged over the length. Left: $R = 50$. Right: $R = 70$.